



Journal of Aerospace Technology and
Management

ISSN: 1948-9648

secretary@jatm.com.br

Instituto de Aeronáutica e Espaço
Brasil

de Oliveira Vale, Tiago; da Costa Villar, Gustavo; Carlos Menezes, João
Methodology for Structural Integrity Analysis of Gas Turbine Blades
Journal of Aerospace Technology and Management, vol. 4, núm. 1, enero-marzo, 2012, pp. 51-59
Instituto de Aeronáutica e Espaço
São Paulo, Brasil

Available in: <http://www.redalyc.org/articulo.oa?id=309426250008>

- How to cite
- Complete issue
- More information about this article
- Journal's homepage in redalyc.org

redalyc.org

Scientific Information System
Network of Scientific Journals from Latin America, the Caribbean, Spain and Portugal
Non-profit academic project, developed under the open access initiative

Methodology for Structural Integrity Analysis of Gas Turbine Blades

Tiago de Oliveira Vale*, Gustavo da Costa Villar, João Carlos Menezes

Instituto Tecnológico de Aeronáutica - São José dos Campos/SP – Brazil

Abstract: One of the major sources of stress arising in turbomachinery blades are the centrifugal loads acting at any section of the airfoil. Accounting for this phenomenon stress evaluation of the blade attachment region in the disc has to be performed in order to avoid blade failure. Turbomachinery blades are generally twisted, and the cross section area varies from the root of the blade to the tip. The blade root shape at the attachment region is of great concern. Stress concentrations are predictable at this contact region. In this paper, a finite element model has been created for the purpose of assessing stress at the joint region connecting the blade to the disc slot. Particular attention was paid to the geometric modeling of the “fir-tree” fixing, which is now used in the majority of gas turbine engines. This study has been performed using the commercial software ANSYS 13.0. The disc and blade assembly are forced to move with a certain rotational velocity. Contact connections are predicted on the common faces of the blade and on the disc at the root. Solutions can be obtained to allow the evaluation of stresses. Results can be compared with the mechanical properties of the adopted material..

Keywords: Stress Analysis, Finite Element Method, Gas Turbine Blade, Fir-tree Joint.

INTRODUCTION

One of the main factors concerning mechanical integrity of aeroengine turbines is the interface region between the blade and the rotor disc. Stresses generated in this region are mainly produced by the centrifugal force resulting from the rotational speed of rotor mass of the blade, thermal stress, and bending loads and torsion due to the gas pressure. According to Meguid *et al.* (2000), the joint between a turbine blade and the disc represents the most critical load path within this assembly, and it is crucial to the operational safety and service life of gas turbine engines.

In order to accommodate safe stresses values in this contact region, an adequate geometry has to be developed for the joint. A variety of methods has been adopted for fastening blades to discs. The dovetail slot type is composed of a single tooth, and this type of fastening is usually used in rotors of compressors and fans, according to Beisheim and Sinclair (2008). Most frequently, fir-tree fasteners are implemented for they provide adequate multiple and larger areas of contact between the blade and the disc, which results in better

stress distribution on the several teeth, according to Kanth (1998).

The present study focused on the study of stresses arising from the centrifugal loadings in a fir-tree joint using a 3D Finite Element model in the commercial code ANSYS 13.0.

Earlier works carried out by Singh and Rawtani (1982a,b) present results of photoelastic stress analysis of fir-tree assemblies. Very frequently, this kind of experimental technique is used to validate numerical results obtained by the Finite Element Method.

In the work of Parks and Sanford (1978), the full distribution of stress field in a dovetail joint of a turbine was assessed using the photoelastic method. The results allowed the removal of material in the interface region and thus obtained 27% reduction in stress concentration, as well as to reduce the weight of the component.

Uchino *et al.* (1986) developed a 3D photoelastic analysis in a dovetail joint of a gas turbine disc groove. The authors presented results of stress variation and compared them with 3D finite element analysis along the thickness. The work shows the influence of the inclination skew angle from 0 to 45°. Results for skew angle of 45° present 2.5 times higher stress compared to the straight skew

Received: 19/09/11. Accepted: 12/11/11

*author for correspondence: tiago.vale@yahoo.com.br/Pç. Mal. Eduardo Gomes, 50. CEP: 12.228-901 - São José dos Campos/SP - Brazil

angle. Therefore, the skew angle of 45° has the higher stress of those analyzed.

Many researches developed structural analysis studies related to dovetail joints through the finite element method. Meguid *et al.* (1996), analyzed the stresses in an aeroengine compressor. The geometry was modeled using the software IDEAS, and the finite element model was created in ABAQUS. The authors showed that the maximum stress occurs just below the lower contact point between the blade and the disc.

Papanikos *et al.* (1998) conducted a stress analysis study at a dovetail joint using the software ANSYS. It revealed that the lowest stress occurs for a 70° contact angle. Another important factor shown is the influence of friction, revealing that in the absence of this factor the maximum stress was 30% higher.

The effect of the skew angle inclination was carried out by Anandavel and Prakash (2010). The study shows that the groove with skew angle of 20° presents a stress two times greater than the straight skew angle, and the stress with friction is about 30% less than frictionless.

Shankar *et al.* (2010) illustrated the stress distribution through 3D finite element analysis of low-pressure steam turbine bladed disc assembly with loading and constant speed of 6,000 RPM in ANSYS 12.0. The results showed that the peak stress of 1,187MPa is seen at blade root fillet pressure face and 1,055MPa at suction side.

Other studies using finite element method were carried out for fir-tree joints. Chan and Tuba (1971) checked the stress in a fir-tree root through finite element method by changing the coefficient of friction and the clearances. Clearance changes showed more significant effects of stress than the coefficient of friction.

Singh and Rawtani (1982a) evaluated the deformation in the bottom tooth of a fir-tree root. In their second work, they (1982b) studied the complete fir-tree root.

Delhelay (1999) performed a thermo-mechanical analysis in the fir-tree root region. This work presented the study of stresses in 2D and 3D geometries, considering non-linear contact conditions. It was concluded that the bottom tooth is subjected to the highest stresses and the coefficient of friction does not significantly alter the stress values.

Meguid *et al.* (2000) evaluated the von Mises stress distribution undertaken of the fir-tree region in aeroengine turbine disc assembly with different geometries, using the software ANSYS. The studies show the influence of the contact angle α , top (γ) and bottom flank angle (β), straight and skew angle, coefficient of friction, and number of teeth.

Results show that the stress peak occurs right below the lower contact point along the bottom tooth of the turbine disc, and the coefficient of friction alters the stress value.

This search for optimized geometries of fir-tree joints has been the main purpose of designers and engineers. Thinking of this, Song *et al.* (2002) developed an optimization program of fir-tree root of a turbine, using a CAD system with several optimization algorithms and stress analysis by finite element method.

A similar work was done by Brujic *et al.* (2010), the author developed an optimization program of the fir-tree root of a gas turbine with automatized results. The program was written in MATLAB, modeled in CATIA, and finite element meshing and stress analysis were generated by PATRAN/NASTRAN.

VALIDATION OF THE METODOLOGY BY 3D FINITE ELEMENT ANALYSIS

Analysis of the dovetail rim region

In this section, the stress distribution was analyzed in the interface region of the blade and disc in a dovetail joint, considering a rectangular geometry for the blade and disc, employing a Finite Element Model. For this task, the commercial software ANSYS 13.0 was used.

Blade-disc dovetail joint is an important component and is usually found in the fan and compressor disc assemblies of aero-engine.

In this study, the 3D model has been created on the software CATIA V5R18. A similar reference model was examined by Papanikos *et al.* (1998), and Anandavel and Prakash (2010). This study is concerned with the validation of the methodology applied in the contact between the disc and blade using contact elements. In addition, a mesh convergence test was carried out to obtain a proper mesh for the model. In the next section, the validation of the method found here will be imposed in the fir-tree joint, which is the main goal of this work.

One may comment on the great difficulty to find in the literature a geometry that represents the interface region between the blade and disc, and results generated by centrifugal loading. The dimensions of the blade geometries and disc developed are presented in Fig. 1.

Boundary conditions

For the present study, the material used was the same employed by Papanikos *et al.* (1998). The properties of the

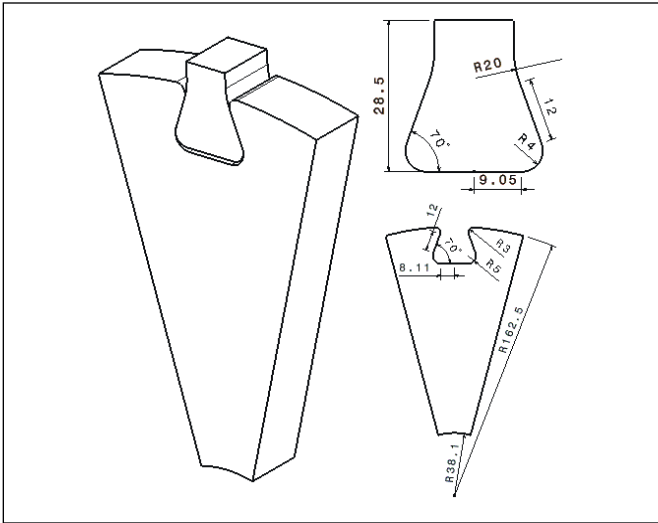


Figure 1. Geometry of dovetail joint.

materials used for modeling the blade and disc were that of titanium alloy Ti-6Al-4V. In this work, the following values were used: Young’s modulus $E=114\text{GPa}$, Poisson’s ratio $\nu=0.33$, and density $\rho=4429\text{kg/m}^3$. All examined models were submitted to centrifugal loading with specific angular velocity, where ω was selected to be 1,000rpm. In view of symmetry of geometry and loading, only one sector of the disc supporting 12 blades was modeled as shown in Fig. 1. This model was imported to ANSYS 13.0 and the cyclic symmetry

tool was used, greatly reducing computational time, compared to a full disc/blades model that would require a much higher computational effort.

Contact elements

The contact surfaces in the dovetail region were modeled using contact elements. The contact region between the blade and the disc is recognized by ANSYS 13.0, at the time the geometry is imported from CAD software. Friction and frictionless conditions were selected on the interface, and Lagrange multiplier method was used to obtain solutions for normal and friction contacts. The dovetail interface was defined as the stiffness matrices of each element is updated at each iteration. Given these definitions, the contact region is considered as a nonlinear contact condition (Fig. 2).

Mesh

There are several methods for discretization available for the generation of finite element meshes in non-linear contact analysis. A free meshing routine was used due to the necessity to model a complex geometry with large transitions in the stress field.

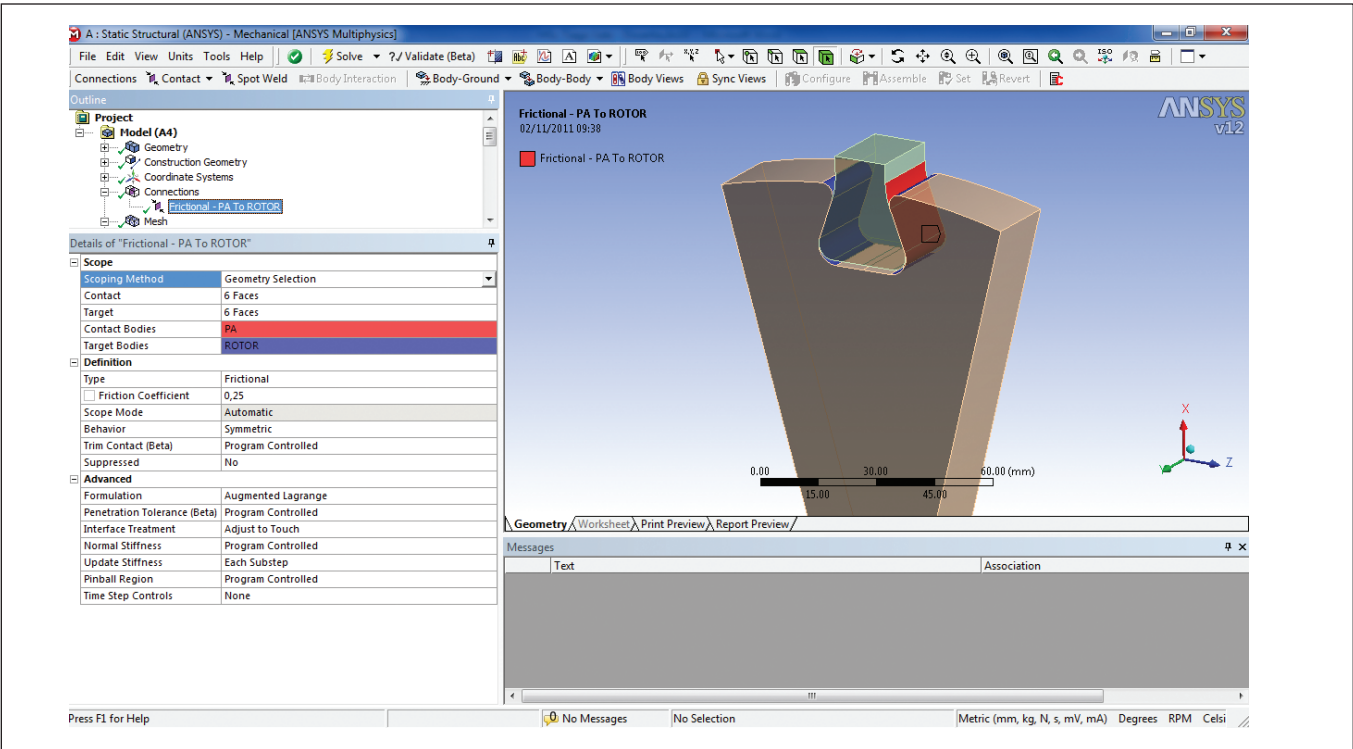


Figure 2.Contact elements.

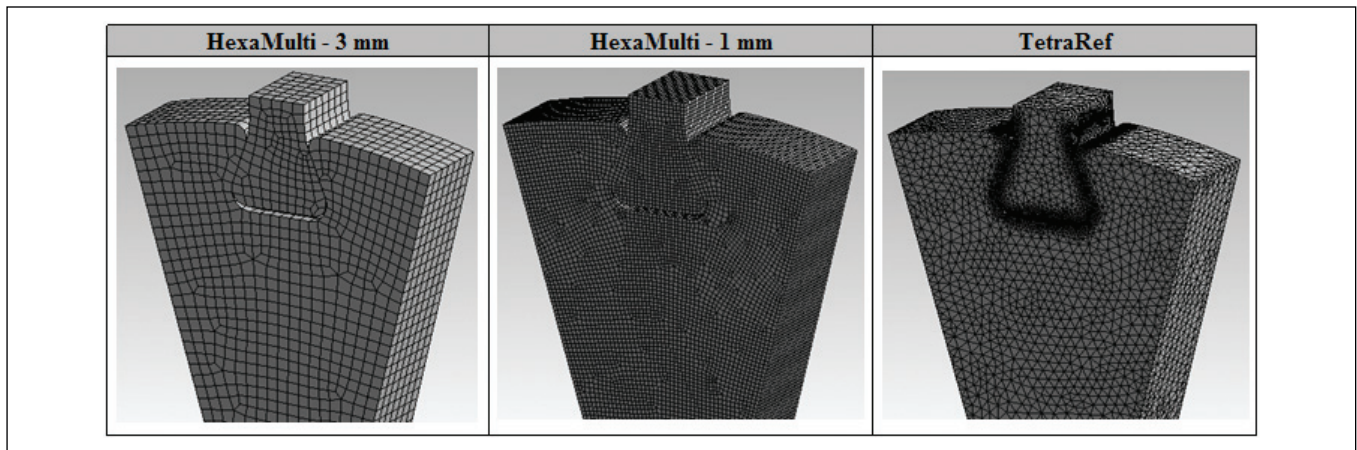


Figure 3. Types of mesh studied in dovetail joint.

Figure 3 shows typical 3D meshes used to test convergence. Three types of meshes have been studied. The meshes HexaMulti 3 and 1mm contain hexahedron elements with 20 nodes per element. A third case, the TetraRef mesh, contains tetrahedral elements with ten nodes, which was refined in the region of contact between the blade and disc. The number of elements and nodes for each mesh type is shown in Table 1.

Table 1. Number of elements and nodes for each type of mesh in dovetail joint.

| | HexaMult 3mm | HexaMult 1mm | TetraRef |
|----------------|--------------|--------------|----------|
| Nº of elements | 5964 | 106172 | 93299 |
| Nº of nodes | 28535 | 455218 | 149580 |

It should be noted that the Von Mises stress values for all figures were normalized by $\sigma/\rho\omega^2a^2$, $\rho\omega^2a^2 = 70.5\text{kPa}$, where ρ is the density of material, ω the angular velocity in rad/s and a is the inner radius of the disc.

The curve represented in Fig. 4 illustrates the normalized Von Mises stress across thickness at the lower contact

line, through interface between the blade/disc for two types of analysis. The three cases described before, considering a coefficient of friction $\mu = 0.25$ and $\mu = 0.0$ (frictionless) were compared to the results published by Papanikos *et al.* (1998).

One may notice a very good agreement between the present result and those reported by Papanikos *et al.* (1998).

Figure 5 shows the normalized Von Mises stresses along the interface between the blade and the disc. In this case, the stresses were obtained by comparing the 3D models studied in this paper with those found in the literature for 2D and 3D models. In these cases, the present results were obtained for coefficient of friction $\mu = 0.25$.

According to this analysis, one may observe that the curves of stresses for HexaMulti 1mm and TetraRef meshes are very close in agreement with the 3D and 2D models analyzed by Papanikos *et al.* (1998). Only the HexaMulti 3mm mesh has not shown good results, it was observed through the peak stresses.

Table 2 shows the percentage differences between the maximum stresses obtained by the several cases with maximum stress used as a reference to validate the applied methodology.

Table 2. Differences in percentage between the maximum stresses.

| Relationship between literature and the meshes studied | Normalized maximum stress along thickness $\mu = 0.25$ | Normalized maximum stress along thickness $\mu = 0.0$ | Normalized maximum stress along interface blade/disc |
|--|--|---|--|
| Papanikos <i>et al.</i> | 26 | 37.14 | 18.4 |
| HexaMult 3mm | 25.7 | 37.56 | 21.7 |
| Difference [%] | 1.15% | -1.14% | -18.16% |
| HexaMult 1mm | 25.26 | 36.9 | 21.27 |
| Difference [%] | 2.85% | 0.64% | -15.85% |
| TetraRef | 26.29 | 37.62 | 19.61 |
| Difference [%] | -1.1% | -1.31% | -6.74% |

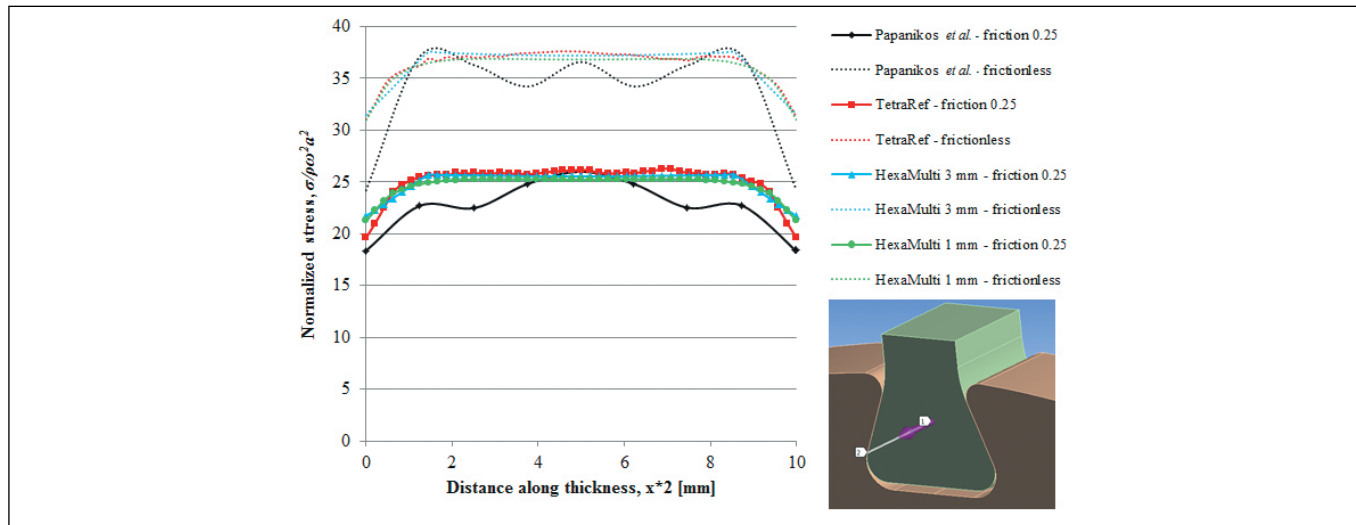


Figure 4. Normalized Von Mises stress along thickness at the lower contact line for different meshes.

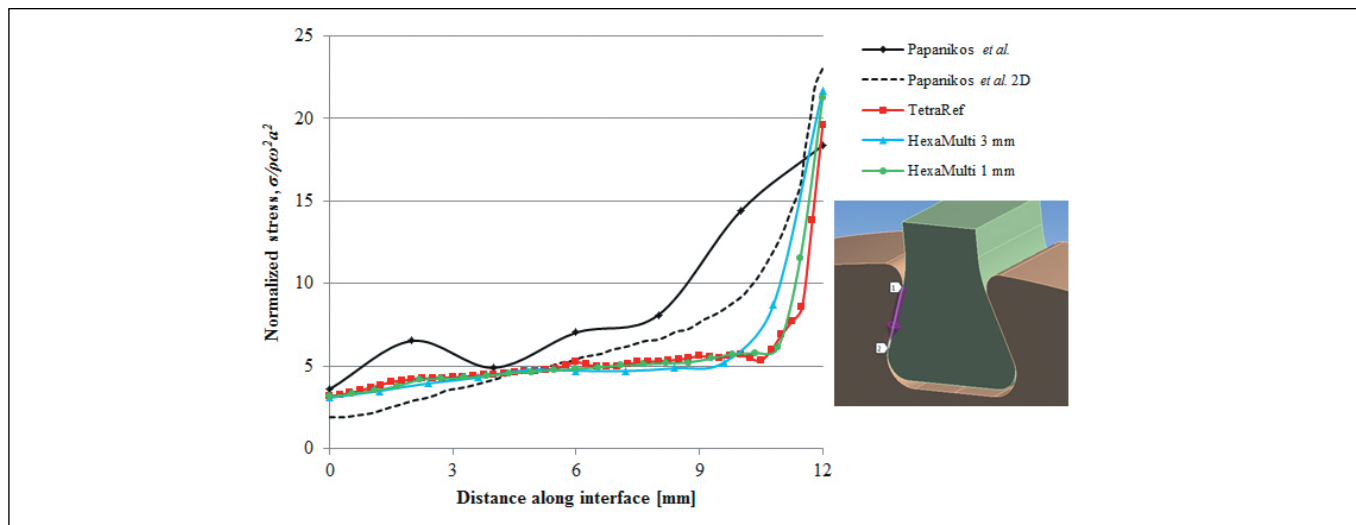


Figure 5. Normalized Von Mises stress along the interface at different meshes.

For each case, the normalized maximum Von Mises stresses are presented. Taking the case presented by Papanikos *et al.* (1998) as a reference, the percentage difference between results is reported.

These results show that stresses across thickness with friction presented a small difference in all cases, and the largest one (2.853%) was found when the HexaMulti 1mm mesh was used for the frictionless case, with the difference being less than 1.31%. However, the analysis of stresses along the interface using the HexaMulti 3mm mesh presents a very high percentage difference of 29.71%, which was not observed for the other two meshes.

It can be concluded that for the methodology used, very consistent and safe results may be obtained.

3D NONLINEAR FINITE ELEMENT ANALYSIS IN FIR-TREE JOINT

In this section, a finite element analysis of the fir-tree region was carried out. Fir-tree joint is very used in the compressor disc assemblies in turbine axial, because it has a larger contact area between the teeth of the blade and the disc, better distributing the stresses.

In this study, the geometrical model created is similar to that used in the works of Venkatesh (1988) and Meguid *et al.* (2000). However, one may observe the lack of more proper reported results, and even for the cited authors, important dimensions for the blade geometry are omitted, making it difficult to find the most perfect reproduction of the earlier proposed geometry. The adopted geometry is as shown

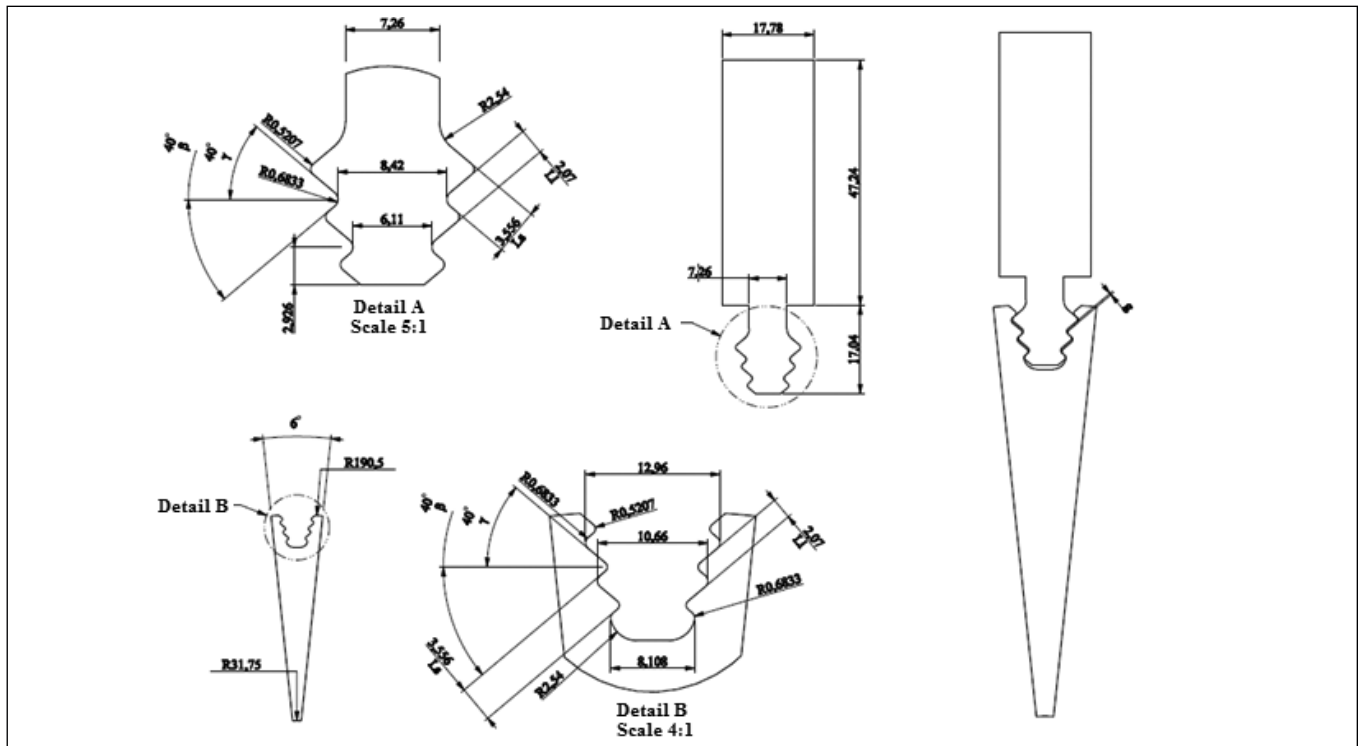


Figure 6. Disc and blade geometry fir-tree joint.

in Fig.6. For the disc and blade, a thickness of 10 mm was adopted. Top and bottom flank angles were taken as $\beta=\gamma=40^\circ$, and rotation speed of the disc was considered as 360rpm. The material properties used for modeling the blade and the disc were that of a typical nickel alloy used in disc design; namely, INCONEL 720. This material is creep and fatigue-resistant. In this work, the following values were used: Young's modulus $E=220\text{GPa}$, 0.2% proof stress ($\sigma=635\text{MPa}$ at 213°C), Poisson's ratio ($\nu=0.29$), density ($\rho=8510\text{kg/m}^3$).

The boundary conditions, contact elements, and mesh applied here, were the same imposed by the dovetail model.

RESULTS

According to the results reported by previous studies of the meshes, we decided to chosen the HexaMulti 1mm and TetraRef meshes. These meshes obtained better results than the HexaMulti 3mm one.

Figure 7 illustrates two cases of the meshes and the number of elements and nodes are shown in Table 3.

Figures 8 and 9 present the normalized Von Mises stress obtained for the two types of mesh, which were previously described compared to results in reported by Meguid *et al.* (2000). Figure 8 presents the stress behavior along the

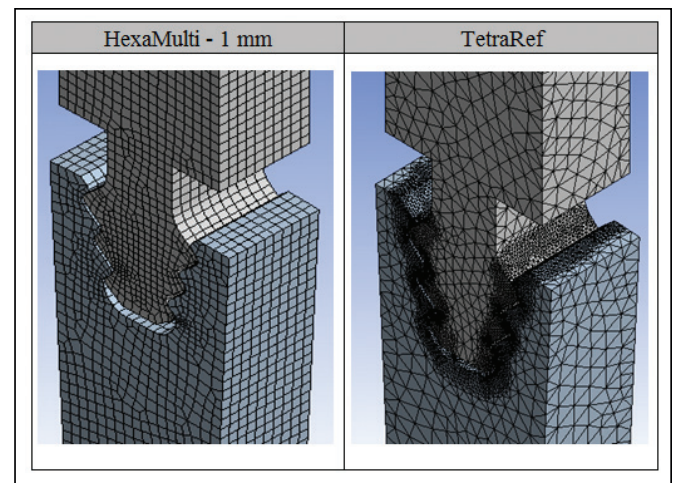


Figure 7. Types of mesh studied in fir-tree joint.

Table 3. Number of elements and nodes for each type of mesh.

| | HexaMult 1mm | TetraRef |
|----------------|--------------|----------|
| Nº of elements | 30160 | 348440 |
| Nº of nodes | 139074 | 598374 |

entire profile of the teeth on the disc side, which reveal higher levels of stress. Figure 9 focuses on the bottom region of the profile. One may notice a better similarity of the normalized Von Mises stress curve obtained by TetraRef mesh with the study

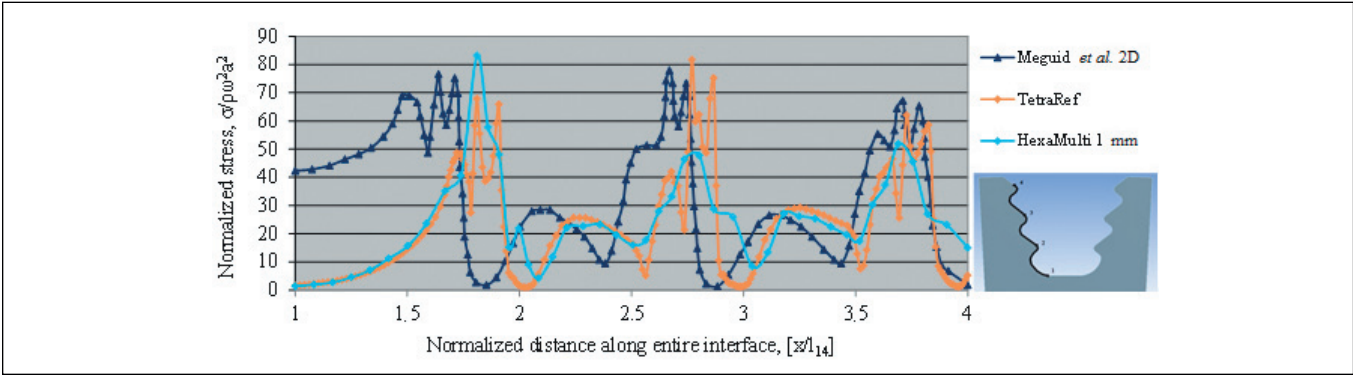


Figure 8. Normalized Von Mises stress along the teeth profile for different meshes.

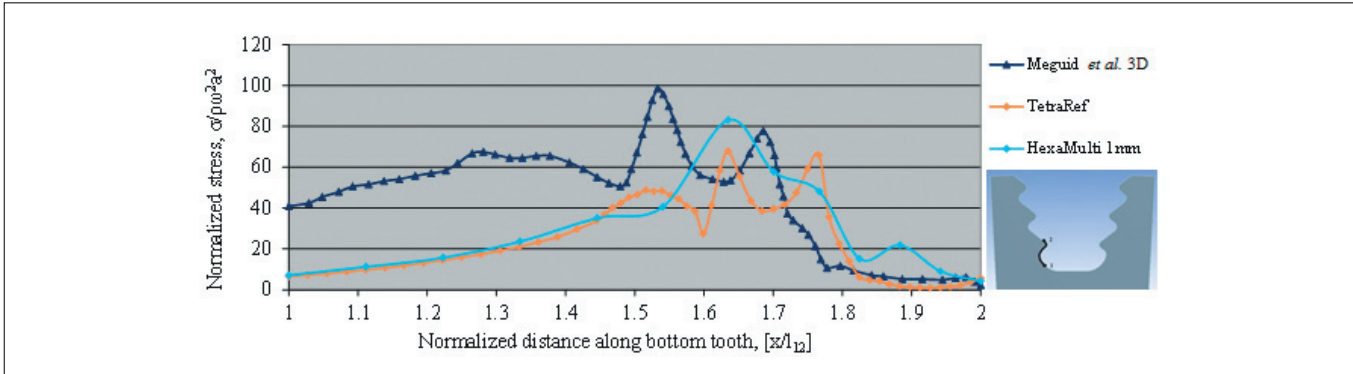


Figure 9. Normalized Von Mises stress along the bottom tooth profile for different meshes.

of Meguid *et al.* (2000). Taking this observation into account, the following studies were performed using TetraRef meshes.

Seven other geometries were generated combining different values of contact angle, top flank angle, superior flank angle, and clearance between the blade and the disc. Table 4 shows the different angles studied. Figures 10 and 11 show the results of stress along the front and back interfaces on the left side of the fir-tree joint.

The graphs show that there is little variation in stresses between the front and back interfaces, because the studied

geometry is symmetrical. Such variations can be seen in Table 5, which presents with details the differences of maximum Von Mises stresses between the front and back sides.

Through this analysis, it was observed that the Case 4 already demonstrated good results in the front, but with considerable variation in the back interface. Case 7 showed the best results with a 10% average in both interfaces, since, without the clearance between the blade/disc, the contact area in the interface region is bigger than the others cases, decreasing stress.

Table 4. Studied geometries.

| Case | Coefficient of friction μ | Contact angle, α | Bottom flank angle, β | Top flank angle, γ | Inferior flank angle, L_i | Superior flank angle, L_s | Clearance between blade/disc |
|------|-------------------------------|-------------------------|-----------------------------|---------------------------|-----------------------------|-----------------------------|------------------------------|
| 1 | 0 | 17.5° | 40° | 40° | 3.556 | 2.08 | 0.38 |
| 2 | 0 | 17.5° | 40° | 30° | 3.556 | 2.61 | 0.38 |
| 3 | 0 | 15° | 40° | 40° | 3.556 | 2.25 | 0.38 |
| 4 | 0 | 15° | 40° | 30° | 3.556 | 2.77 | 0.38 |
| 5 | 0 | 20° | 40° | 40° | 3.556 | 1.89 | 0.38 |
| 6 | 0 | 20° | 40° | 30° | 3.556 | 2.43 | 0.38 |
| 7 | 0 | 15° | 40° | 30° | 3.556 | 2.77 | 0 |

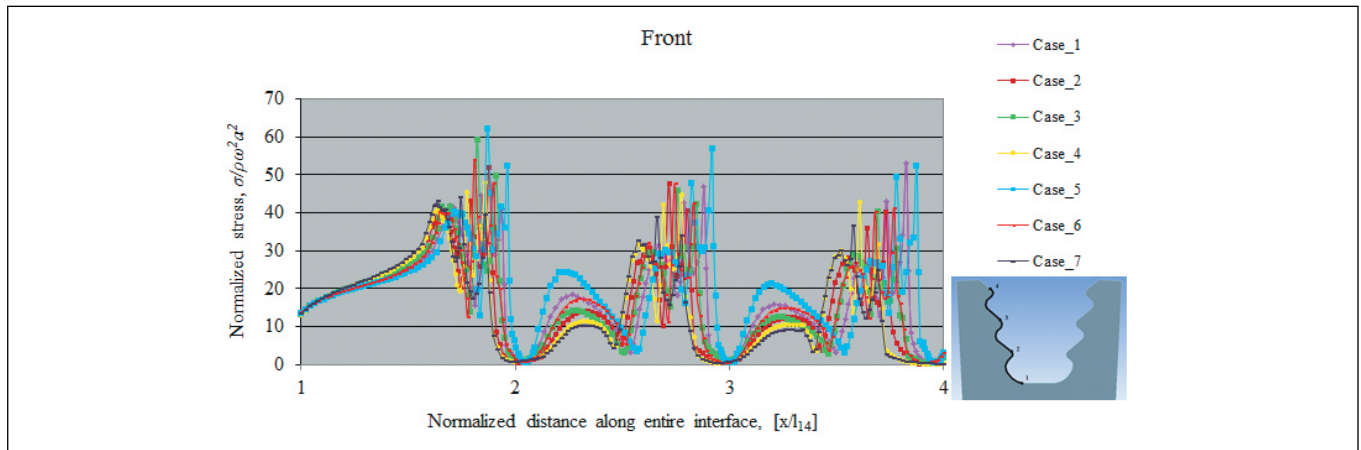


Figure 10. Normalized Von Mises stress along the teeth profile for different meshes on the front side for several cases.

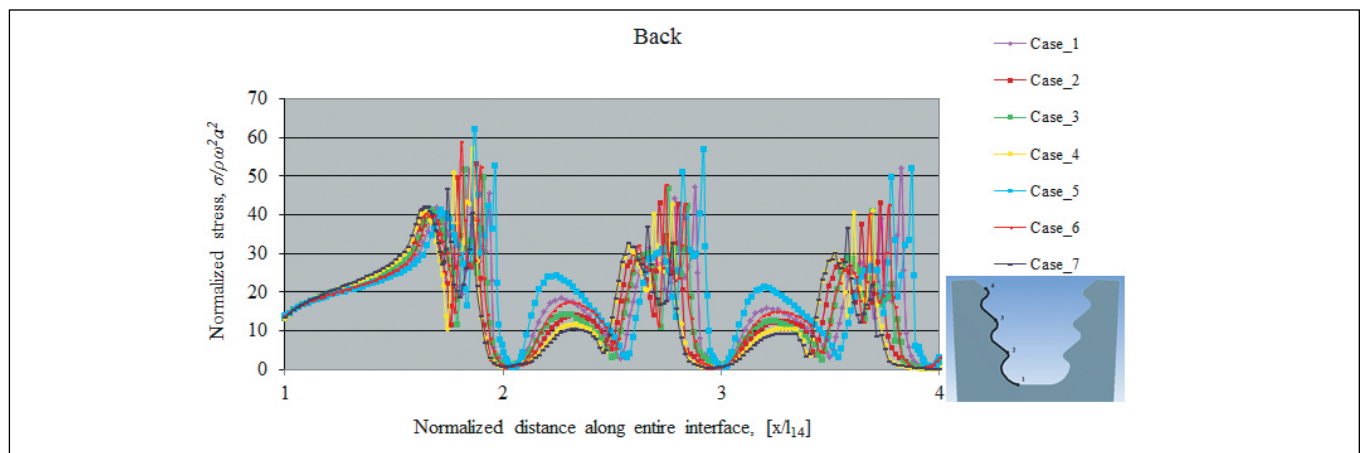


Figure 11. Normalized Von Mises stress along the teeth profile for different meshes on the back side for several cases.

Table 5. Maximum normalized Von Mises stress for the cases analyzed.

| Normalized maximum stress along entire interface $[x/l_{14}]$ | | | | |
|---|-------|--------|-------|------------|
| | Front | | Back | Difference |
| case 1 | 53.15 | case 1 | 52.07 | -2.02% |
| case 2 | 52.03 | case 2 | 53.36 | 2.56% |
| case 3 | 59.31 | case 3 | 51.84 | -12.6% |
| case 4 | 48.1 | case 4 | 57.41 | 19.4% |
| case 5 | 62.32 | case 4 | 62.25 | -0.12% |
| case 6 | 54.03 | case 6 | 58.94 | 9.08% |
| case 7 | 44.3 | case 7 | 46.73 | 5.5% |

CONCLUSIONS

Results from this paper revealed what may be commented as follows:

- the maximum stress value occurs for Case 5, which shows that angles β and $\gamma = 40^\circ$ are not appropriate;

- the minimum stress occurs with a contact angle between 15° and 17.5° ;
- stresses between the front and back region do not vary greatly, except for Case 4.

This study shows the importance of calculating the clearance between the teeth of the blade and the disc, for the calculation of thermal expansion of the bodies indicates the smallest possible value of clearance, thus obtaining a lower stress for the geometry to be developed. However, this factor was not evaluated in this study.

Future papers should clarify the influence of the clearance on the stress values under conditions of thermal expansion and coefficient of friction with variation between 0.0 and 0.5.

The presented model uses the commercial code ANSYS 13.0, which provides several characteristic tools. Among them, there is the possibility of analyzing structures under centrifugal loading. Another useful tool is the friendly interface for modeling contact elements, which is fundamental for this type of analysis.

The present work is a preliminary study of the fir-tree joint between blades and disc. Much more effort must be performed in order to offer the optimum geometry for more general cases.

REFERENCES

- Anandavel, K. and Prakash, R.V., 2010, "Effect of three-dimensional loading on macroscopic fretting aspects of an aero-engine blade-disc dovetail interface", Tribology International.
- Beisheim, J.R. and Sinclair, G.B., 2008, "Three-Dimensional Finite Element Analysis of Dovetail Attachments With and Without Crowning", Journal of Turbomachinery, Vol.130, No. 2.
- Brujic, D. *et al.*, 2010, "CAD based shape optimization for gas turbine component design", Struct Multidisc Optim, Vol. 41, No. 4, pp. 647-659.
- Chan, S.K. and Tuba, I.S., 1971, "A finite element method for contact problems of solid bodies - Part II. Application to turbine blade fastenings", International Journal of Mechanical Sciences, Vol.13, No. 7, pp. 627-639.
- Delhelay, D. S., 1999, "Nonlinear Finite Element Analysis of the Coupled Thermomechanical Behaviour of Turbine Disc Assemblies", Thesis University of Toronto. Toronto, pp. 95.
- Kanth, P.S., 1998, "2D & 3D FE analysis of fir-tree joints in aeroengine discs", Thesis University of Toronto.
- Meguid, S.A., *et al.* 2000, "Finite element analysis of fir-tree region in turbine discs", Finite Elements in Analysis and Design, Vol. 35, No. 4, pp. 305-317.
- Meguid, S.A., *et al.* 1996, "Theoretical and experimental studies of structural integrity of dovetail joints in aeroengine discs", Journal of Materials Processing Technology, Vol. 56, No. 1-4, pp. 668-677.
- Papanikos, P., *et al.* 1998, "Three-dimensional nonlinear Finite element analysis of dovetail joints in aeroengine discs", Finite Elements in Analysis and Design, Vol. 29, No. 3-4, pp.173-186.
- Parks, V.J. and Sanford, R.J., 1978, "Photoelastic and Holographic Analysis of a Turbine-engine Component", Experimental Mechanics, Vol.18, No. 9, pp. 328-334.
- Shankar, M. *et al.* 2010, "T-root blades in a steam turbine rotor: A case study", Engineering Failure Analysis, Vol.17, pp. 1205-1212.
- Singh, G.D. and Rawtani, S., 1982a, "Fir tree fastening of turbomachinery blades - I deflection analysis", International Journal of Mechanical Sciences, Vol. 24, No. 6, pp. 377-384.
- Singh, G.D. and Rawtani, S., 1982b, "Fir tree fastening of turbomachinery blades - II step load analysis", International Journal of Mechanical Sciences, Vol. 24, No. 6, pp. 385-391.
- Song, W. *et al.*, 2002, "Turbine blade fir-tree root design optimisation using intelligent CAD and finite element analysis", Computers & Structures, Vol. 80, No. 24, pp. 1853-1867.
- Uchino, K. *et al.*, 1986, "Three dimensional photoelastic analysis of aeroengine rotary parts", Proceeding of the International Symposium on Photoelasticity, Tokyo, Japan, pp. 209-214.
- Venkatesh, S., 1988, "Structural integrity analysis of an aeroengine disc", Thesis Cranfield Institute of Technology.

